Journal of Magnetic Resonance 212 (2011) 274–279

Contents lists available at ScienceDirect

Journal of Magnetic Resonance

journal homepage: www.elsevier.com/locate/jmr

A mixed basis approach in the SGP-limit

Matias Nordin [a,*], Martin Nilsson-Jacobi [b], Magnus Nydén [a]

[a] Applied Surface Chemistry, Department of Chemical and Biological Engineering, Chalmers University of Technology, 41296 Gothenburg, Sweden
[b] Complex Systems Group, Department of Energy and Environment, Chalmers University of Technology, 41296 Gothenburg, Sweden

ARTICLE INFO

Article history:
Received 12 April 2011
Revised 1 July 2011
Available online 12 July 2011

Keywords:
NMR
SGP-limit
Narrow pulse approximation
Restricted diffusion
Initial slope
Matrix formulation
Laplace operator
Perturbation method
Geometry
Poisson's equation

ABSTRACT

A perturbation method for computing quick estimates of the echo decay in pulsed spin echo gradient NMR diffusion experiments in the short gradient pulse limit is presented. The perturbation basis involves (relatively few) dipole distributions on the boundaries generating a small perturbation matrix in $O(s^2)$ time, where s denotes the number of boundary elements. Several approximate eigenvalues and eigenfunctions to the diffusion operator are retrieved. The method is applied to 1D and 2D systems with Neumann boundary conditions.

1. Introduction

NMR-methods provide an arsenal of tools to study restricted diffusion [1–3] where not only mass transportal properties such as flow and diffusion can be studied [4–7] but also characteristics of the material [8–11]. Commonly used for diffusion studies is the pulsed gradient spin-echo (PGSE) NMR technique where the particle positions are labeled by a magnetic field gradient [12]. Position labeling is commonly performed by finite-length magnetic field gradient pulses and the theory for this experiment is described by the Bloch–Torrey equations [13]. In the short gradient pulse (SGP) limit however, the spin-echo decay simplifies to a Fourier transform over the propagator [3]. The SGP-limit is therefore commonly used to describe the diffusion process when the geometric length scales of the material are longer than the effective gradient length scales as given in the q-vector approach [14–17]. In heterogeneous materials the spin-echo decay normally results in a function that can be described by a sum of exponentially decaying functions, resulting in a rather featureless form. However, in structurally well-defined materials, such as packed mono-disperse micrometer sized beads, it can display detailed features from which material structure details can be obtained [18–20,11,14,21]. In addition, in the SGP-limit, the initial slope of the spin-echo decay always conveys information of the mean square displacement independent on material homogeneity/heterogeneity. It is thus of interest to calculate a spin-echo decay from homogeneous and heterogeneous materials, in order to gain knowledge about the dependence between material structure and diffusion. The naive approach to calculate the echo decay in the SGP-limit is done by diagonalizing the diffusion operator. In this paper we develop a perturbation technique to calculate rough, but quick estimates of the echo decay, based on approximate eigenfunctions of the diffusion operator. These approximate eigenfunctions separates free diffusion and the influence of the material. Interesting features of the material can thus be analyzed in detail, also for large scale systems.

2. Theory

In the short gradient pulse limit the echo decay is described by the so called master equation, a Fourier transform over the propagator [6,12,22]

$$E(q,t) = \frac{1}{V}\langle q|P(r,r',t)|q\rangle. \tag{1}$$

The volume term $\frac{1}{V}$ arise from the assumption that the initial positions of the particles are equally distributed among the volume of the sample and $\langle q| = e^{i2\pi qz}$, where q is a real and the applied gradient is in the z-direction. The propagator in Eq. 1 denotes the ordinary diffusion propagator [22], which can be expanded in eigenfunction/eigenvalue pairs [23,22] as

* Corresponding author. Fax: +46 31160062.
E-mail address: matias@chalmers.se (M. Nordin).

1090-7807/$ - see front matter © 2011 Elsevier Inc. All rights reserved.
doi:10.1016/j.jmr.2011.07.002

$$P = \sum_{i=0}^{\infty} |i\rangle\langle i| e^{-t\lambda_i}.$$

The eigenequation for the eigenfunction/eigenvalue pairs is written as

$$L|i\rangle = \lambda_i |i\rangle, \tag{2}$$

where L denotes the effective diffusion operator associated with the boundary conditions (which will be defined in detail below). Note that the master equation (Eq. 1) can be written as

$$E(q,t) = \frac{1}{V}\sum_{i=0}^{\infty} e^{-t\lambda_i} |\langle q|i\rangle|^2 \tag{3}$$

i.e. the echo decay is defined by the overlap between incoming (Fourier) modes $\langle q|$ and the eigenfunctions $|i\rangle$ of the diffusion operator L, weighted by the time-dependent term $e^{-t\lambda_i}$. In general, Eq. 3 must be solved using numerical methods, since the eigenfunctions of the diffusion operator are known only for simple geometries. In the case of free diffusion using periodic boundary conditions on the computational cell, the diffusion operator reduces to the Laplace operator Δ. We note that in this situation, the eigenfunctions to the Laplace operator and the incoming modes $\langle q|$ in Eq. 3 coincide, when q is integer valued [24]. From now on we will restrict ourselves to the set of integer valued q and we denote the associated eigenvalues to the free diffusion problem by λ_q.

We write the diffusion operator as

$$L = \Delta - S \tag{4}$$

where S denotes an operator defining the boundary conditions. We will refer to S as the surface operator and view its presence as a perturbation on the free diffusion problem $\Delta|q\rangle = \lambda_q|q\rangle$. The problem here is that, viewed as a perturbation on the Laplace operator, the norm of S is not small and standard perturbation techniques are not applicable. Now we will show that one can still use a perturbative approach, by using a "mixed basis" which captures the relevant information from the Laplace operator: describing free diffusion, and the surface operator: describing the boundaries.

Since the unperturbed problem ($S = 0$) reduces to Laplace equation it is evident that part of the perturbation basis need to consist of a set of integer valued $|q\rangle$, for a correct solution in absence of S. By recalling the form of Eq. 3 we are motivated to find some set of functions *orthogonal to* $|q\rangle$ describing the influence of the surface operator S. The eigenfunctions of the diffusion operator would then be approximated by linear combinations of $|q\rangle$ and these unknown vectors. Due to this orthogonality condition, the calculation of the echo decay in Eq. 3, would then reduce to a calculation of the contribution of the current $|q\rangle$ to the linear combination spanning the eigenfunctions and the associated eigenvalues in the following manner:

$$E(q,t) \approx \frac{1}{V} e^{-t\lambda'} \langle q| \left(\sum_q \alpha_q |q\rangle + \cdots \right) = \frac{1}{V} e^{-t\lambda'} |\alpha_q|^2. \tag{5}$$

The weights α_q are influenced by the surface operator S and the dots denote the terms comprising of the unknown surface vectors. λ' denotes the approximate eigenvalues of L formed by the inner product of the approximate eigenfunctions and the diffusion operator (to be defined below). We will now expand on this idea and show how to construct these "unknown" surface vectors.

We construct S by assuming Neumann conditions at the boundary Ω

$$\hat{n} \cdot \nabla \phi(\omega \in \Omega, t) = 0, \tag{6}$$

for the (unknown) solution $\phi(r,t)$. The operator S equals $\hat{n}\cdot\nabla$, and acts as a directional derivative on Ω. Each eigenfunction of S consist of two $\delta(r-\omega)$-functions with sign change over Ω and it is clear

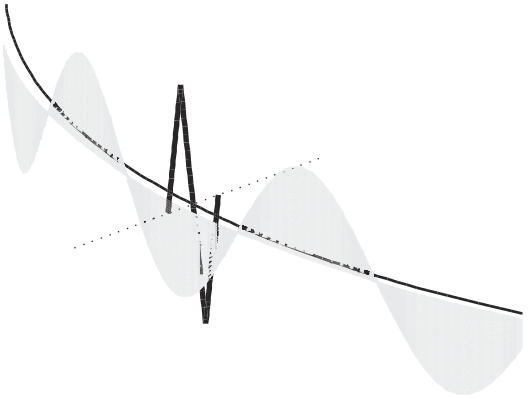

Fig. 1. The figure shows a conceptual representation of a boundary Ω (thin solid line) and an eigenfunction to S (thick solid line), which consists of two delta-functions with different sign over the boundary, as a dipole pointing in the direction of the normal to the boundary (dotted line). The grey shaded area show an example of a Fourier mode which span the exterior side of the boundary and thus sets the amplitude of the exterior delta-functions. Due to the dipole nature of the eigenfunctions to S, a Fourier mode of opposite sign span the interior side of the boundary (not shown in the figure) and the two Fourier modes together makes an example of a surface distribution σ_s (c.f Eq. 7).

that standard perturbation techniques will not work, as the norm of S is large in the Laplace basis. By the form of the eigenfunctions to S we will refer to them as dipoles. Now we Fourier expand the eigenspace of S, with sign change over Ω to preserve the dipole form and denote such surface Fourier modes by σ_s (see Fig. 1 for a conceptual representation). If the surface is smooth, a Fourier expansion on the boundary captures incoming waves $\langle q|$ of about the same wave numbers. This means that for a truncated set of Fourier modes $\{\langle q \mid \}_{q=1}^{N}$ in the low q-regime, a set of low wave-number surface modes suffices. We denote the number of such surface modes by M. The corresponding surface functions $|s\rangle$ are then calculated by solving Poisson's equation

$$|s\rangle = \int_{\Omega} \frac{1}{|r-\omega|} \sigma_s(\omega)\, d\omega \tag{7}$$

where in two dimensions the kernel is replaced by $\log|r-\omega|$. The approximate solutions to the diffusion problem (cf. Eq. 2) $|i'\rangle$ can then be written as linear combinations of eigenfunctions to the Laplace operator $|q\rangle$ and solutions $|s\rangle$ to Poisson's equation (Eq. 7)

$$|i\rangle \approx |i'\rangle = \sum_q^N \alpha_q |q\rangle + \sum_s^M \beta_s |s\rangle \tag{8}$$

and the approximate eigenvalues can be formed by $\lambda' = \langle i'|(\Delta - S)|i'\rangle$. This linear combination does not bear sense if $N \to \infty$, as of course $\{|\, q\rangle\}_{q=0}^{\infty}$ already form complete set. If we however restrict ourselves to a subset of eigenfunctions of Δ, $N < \infty$, the complementary basis spanned by $|s\rangle$ is interesting and proposes a perturbation technique [1]. The outline of the mixed basis approach can also be found in Ref. [25].

Although the surface distributions $\sigma_s(\omega)$ are chosen to be orthogonal, the corresponding $|s\rangle$ will not be, but more importantly they nor will be orthogonal to $|q\rangle$. Hence, before the perturbation matrix is formed, an orthogonalization procedure of the surface modes $|s\rangle$ is needed

$$|s\rangle \to |s_\perp\rangle \tag{9}$$

The resulting vectors $|s_\perp\rangle$ are orthogonal to each other and also to the subset of free harmonic functions $\{|\, q\rangle\}_{q=1}^{N}$. The orthogonalization

[1] This restriction also connects naturally with the experimental NMR setup, where the range of q-vectors is not complete but restricted by the gradient strength available.

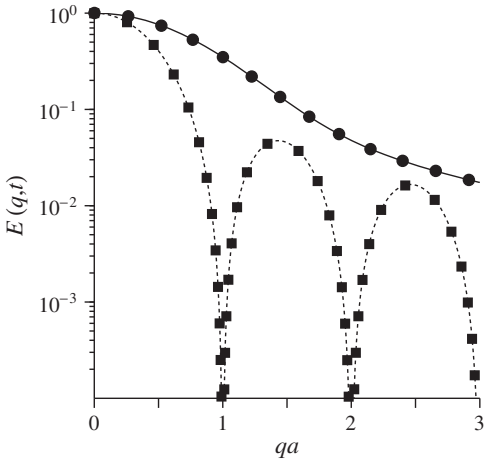

Fig. 2. The figure shows echo decays for diffusion between two plates, separated by distance a. The real echo decay is calculated using Eq. 3 with the full spectrum of the diffusion operator L for time $t = 100$ (•). The approximate echo decay for the corresponding time is calculated using $N = 10$ eigenfunctions to the Laplace operator Δ and $M = 1$ surface function (solid line). Also shown is the infinite time solution $E(q,\infty) = |\mathrm{sinc}(\pi q l)|^2$ (■) and the approximate infinite time solution (dashed line) using the same perturbation basis as for the $t = 100$ signal. The approximate signals coincide well with expected results (the relative error is of order 10^{-4}).

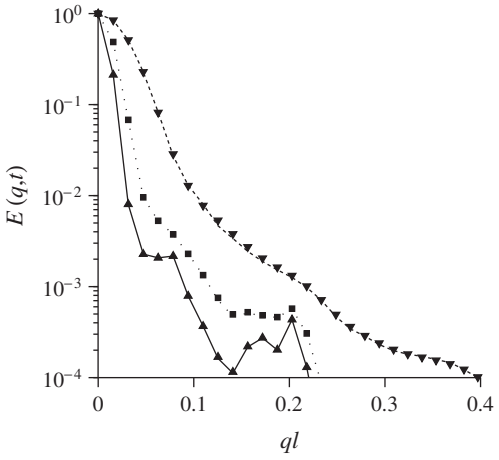

Fig. 4. The figure shows echo decays for the 2D-example of randomly distributed discs (see Fig. 3). The real echo decay (calculated using Eq. 3) is shown for times $t = 200$ (▼), $t = 900$ (■) and $t = 2000$ (▲). The approximate echo decay is calculated using $N = 150$ eigenfunctions to the Laplace operator Δ and $M = 280$ surface functions and is shown for $t = 200$ (dashed line), $t = 900$ (dotted line) and $t = 2000$ (filled line). The box side length is $l = 200$. The relative error of the approximate echo decays is of order $\sim 10^{-3}$. Note that the approximative echos are calculated only at the corresponding q-values but lines are drawn between these, for visualization.

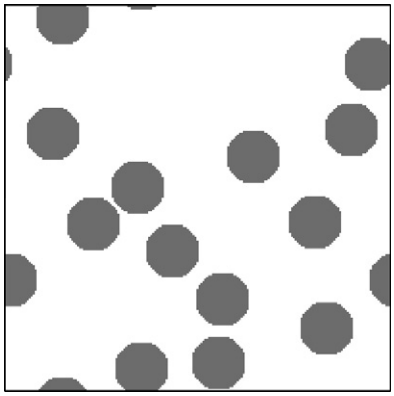

Fig. 3. The figure shows a 2D-system consisting of randomly distributed discs of equal radius. The system consist of 4×10^4 grid points and Neumann boundary conditions separates the void space (white region) from structure (grey region). Fig. 4 shows the real and approximate echo decay for different times.

procedure (e.g Gram–Schmidth) can be performed on the surface only by the following observations. Firstly, the scalar product between a harmonic function and a surface function $|s\rangle$ can be performed as a surface calculation

$$\langle q|s\rangle = \frac{1}{\lambda_q}\langle q|\sigma_s\rangle$$

since Δ is self-adjoint. Furthermore, the scalar product between two solutions to Poisson equation can be treated as follows:

$$\begin{aligned}\langle s|s'\rangle &= \int_V \int_\Omega \frac{\sigma_s(\omega)}{|r-\omega|}\,d\omega \int_\Omega \frac{\sigma_{s'}(\omega')}{|r-\omega'|}\,d\omega'\,dr \\ &= \int_\Omega \sigma_s(\omega)\sigma_{s'}(\omega')\Theta(\omega,\omega')\,d\omega\,d\omega' \qquad (10)\end{aligned}$$

where the resulting integrals ω and ω' are over the surface only. The interchange of the integration variables is valid provided that the unit cell is neutral [26] and the resulting function $\Theta(\omega,\omega')$ can be pre-calculated! Importantly the function Θ only depends on the unit cell size and number of dimensions and thus needs only to be calculated once and used as a look-up table. Furthermore, by noting that both

$$(\Delta - S)|s_\perp\rangle$$

and

$$(\Delta - S)|q\rangle$$

only need to be calculated over the surface, the resulting perturbation matrix is quickly accessible and is of size $(N+M)\times(N+M)$. The perturbation matrix has the following form:

$$A_{i,j} = \langle i|(\Delta - S)|j\rangle$$

where i and j range over all perturbation vectors, i.e. $\{\langle q\,|\,\}_{q=1}^{N}$ and $\{\langle s_\perp\,|\,\}_{s=1}^{M}$. The scalars α_q in Eq. 5 as well as the approximate eigenvalues can be retrieved by diagonalization of the small perturbation matrix A. We denote the eigenfunctions of the perturbation matrix by $|k\rangle$. It may be noted that when $t \to \infty$ the echo decay reduces to the first column of the perturbation matrix.

3. Notes on implementation

In this section we summarize the mixed basis method and suggest practical steps of implementation. The method can be summarized in the following manner:

1. Formation of S and the surface Fourier modes.
2. Solution of Poisson equation for the surface modes.
3. Orthogonalization of the surface modes.
4. Formation and diagonalization of the perturbation matrix A.
5. Formation of the echo decay from eigenvalues to A and weights α_q.

In the first step S and the Fourier modes spanning the boundaries are formed, using the coordinates of the boundary elements. In two dimensions it is straight forward to parameterize Fourier modes spanning the boundaries. Due to the form of the eigenvectors to S, an inner and outer Fourier mode is formed, with sign change over the boundary. Importantly in this step, the computational cell must be charge neutral $\int \sigma_s(r)\,dr = 0$. In this paper the

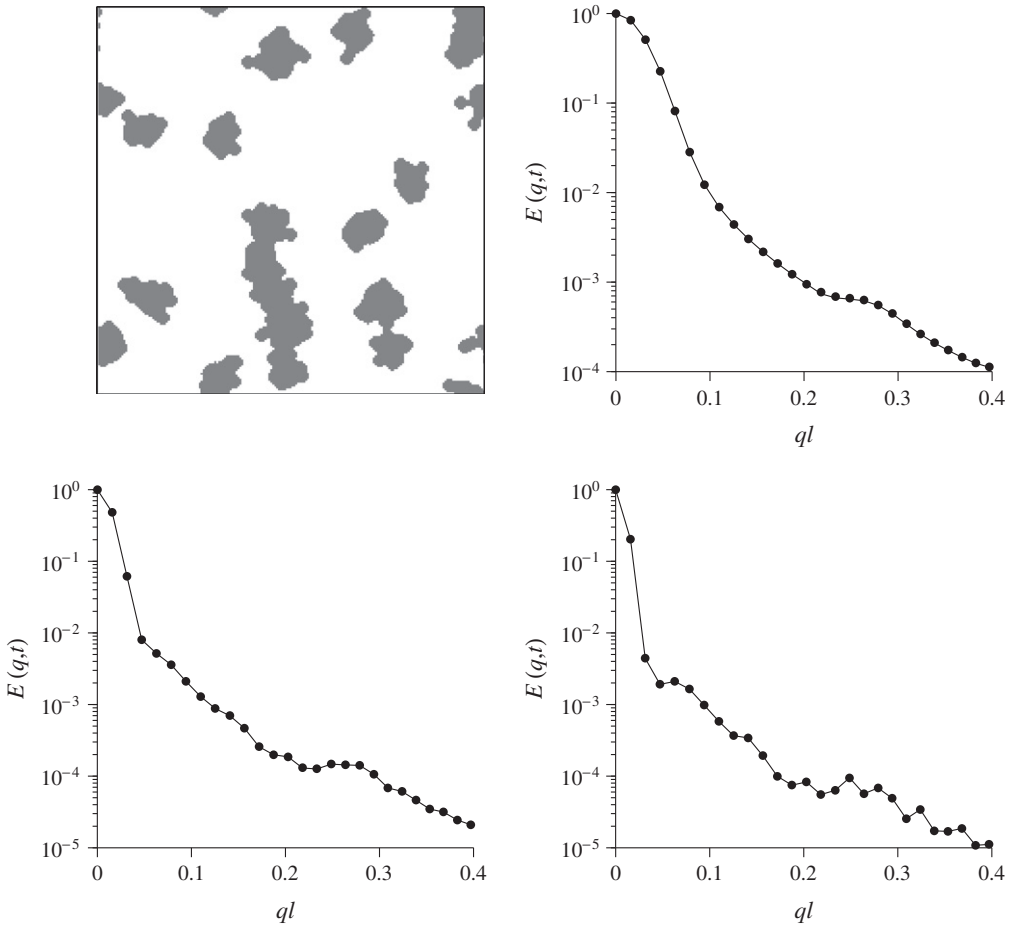

Fig. 5. Echo decays for the model shown in top left image for times $t = 200$ (top right), $t = 900$ (bottom left) and $t = 2000$ (bottom right). The real echo decay $E(q, t)$ is calculated using Eq. 3 (•) and the approximative echo decay is calculated using $M = 100$ surface functions and the first $N = 100$ eigenfunctions of Δ (solid line). Note that the approximative echo is calculated only at the corresponding q-values but the solid line is drawn between these, for visualization. $l = 200$ denotes the box side length. The relative error of the approximative echo decay is of order $\sim 10^{-2}$.

surface Fourier modes was formed by first: calculation of the first (smallest eigenvalues) eigenvectors to a Laplace operator defined on the (outer) boundaries and secondly: forming the Fourier mode spanning the inner boundary directly by using the values at the outer boundaries. Since the surface Laplace operator is sparse and symmetric the diagonalization can be made using standard Lanczos techniques where each iteration is performed in linear complexity with respect to the number of boundary elements $O(s)$. The reason that this approach was used is that it is general and works for any number of dimensions. In the second step the Poisson equation is solved for each surface mode, generating the surface modes $|s\rangle$. The Poisson equation can be solved in linear complexity $O(s)$ using Fast Multi Pole (FMM) techniques [27] due to the fact that the solution is only needed at the surface elements. In the third step the surface modes $\{|s\rangle\}_{s=1}^{M}$ are orthogonalized with respect to each other, and also to the set of free modes $\{|q\rangle\}_{q=1}^{N}$. Using the Θ-operator and the properties of the functions used (described in the section theory) this can be performed on the surface only in $O(s^2)$ complexity. The reason for the square term is the double integral in Eq. 10. It is possible that this can be enhanced further to linear $O(s)$ complexity using combined Ewald summation techniques and FMM methods [28]. In the fourth step the perturbation matrix A is formed using Eq. 2. It is fully populated, but of size $(N + M) \times (N + M)$ and hence the complexity for diagonalizing A can be disregarded. The eigenvalues to A are approximations of the eigenvalues to the original operator L and the associated eigenvectors of A give the weights to the linear combinations of the basis functions approximating the eigenvectors to L according to Eq. 8. In the fifth step the weights of the $|q\rangle$-functions retrieved from the eigenvectors to A are used together with the approximate eigenvalues to form the echo decay using Eq. 5.

4. Results

The perturbation basis has been validated in several trivial and non-trivial domains with good results. Three examples are presented here and in all examples the free space diffusion constant is set to unity.

The first example consists of diffusion between two plates separated by a distance a, a well studied situation for which an analytic expression is known [29,15,30]. A standard finite difference approach is used with a grid spacing $h = a/50$. The perturbation basis consist of $N = 10$ eigenfunctions to the Laplace operator Δ, and one dipole function representing the boundary ($M = 1$). The echo decay is shown in Fig. 2 for $t = 100$ and $t = \infty$ together with the real SGP-signal calculated from the eigenfunction expansion of L and the analytical infinite time solution $E(q,t \to \infty) = |\mathrm{sinc}(\pi q l)|^2$ [2]. The relative error of the approximate echo decay is of order $\sim 10^{-4}$ for this perturbation basis and relative error of the apparent diffusion constant, estimated from the initial slope of the echo decay [31], is also of order $\sim 10^{-4}$.

The following two examples consist of two-dimensional systems using 4×10^4 grid points. Periodic boundary conditions are

used on the computational cell, which has a side length $l = 200$. Neumann boundary conditions separate the void space (white regions) and the structure (grey regions) and the echo decays are calculated in the void space. The dipole distributions for the boundaries are calculated by diagonalizing the finite difference approximation on the boundary yielding Fourier modes spanning the surface and sign change over the domain preserve the dipole form. The first such example consist of randomly distributed discs with equal radius (see Fig. 3). Fig. 4 shows the real and approximate echo decays for times $t = 200, 900, 2000$. The real echo decay is calculated with Eq. 3 using the 280 first eigenfunctions/eigenvalues to L, which gives an error $<10^{-9}$ for $t > 200$. The approximate echo decay is calculated using the first $N = 150$ eigenfunctions to Δ and 20 surface Fourier modes per disc are used, in total $M = 280$ surface functions represent the boundaries. The relative error of the echo decay is of order $\sim 10^{-3}$.

The last example consists of diffusion in a more interesting 2-dimensional model. The model is generated by a parent/child process [32], where parents are created randomly using a uniform distribution and children are distributed around each parent using a Gaussian distribution. The pixel positions of the children then represent the material. The number of parents/children and the distribution parameters can be varied and the space of geometries is rich. Although such geometries work well in discrete case, they can of course not be spanned by Fourier modes in the continuous limit. Fig. 5 shows an example of one such geometry and echo decays calculated for times $t = 200, 900, 2000$. The perturbation matrix is calculated using the $N = 100$ first eigenfunctions to Δ and $M = 100$ surface vectors. In the calculation of the real echo decay the first 230 eigenfunctions corresponding to the void space are used, which gives an error of order $<10^{-9}$ for $t > 200$. The relative error of the approximative echo decay is of order 10^{-2}.

5. Conclusions

We have shown that for diffusion problems with Neumann boundary conditions the echo decay in the SGP-limit can be calculated via a perturbation method with a mixed basis. Approximate echo decays are presented together with analytic and real echo decays (calculated from the eigenfunction expansion of the diffusion operator) for trivial and non-trivial geometries and the relative error of the echo decay is small. The mixed basis consist of (analytically known) eigenfunctions to the Laplace operator and solutions to Poisson's equation with dipole distributions on the boundary. Relatively few base vectors are needed for good result, resulting in a quickly accessible perturbation matrix. The method is formulated on the boundary, apart from a volume dependent function, which however is geometry independent and can be pre-calculated using standard Ewald summation techniques, saved to disk, and used as a lookup table for arbitrary geometries. This reduces the calculations of approximate propagators and echo decays in the SGP-limit to a computational complexity of $O(s^2)$, where s is the number of surface elements. As one may view the scalar product between the surface modes as a potential interaction between the charges, where the Θ-function denotes the potential, the method could perhaps even be reduced to a linear time complexity $O(s)$ by combining Ewald summation techniques and Fast Multi Pole methods. This is currently a work in progress.

As the approximate eigenfunctions not fully compensate for the Neumann conditions on the boundaries a resonance effect has been observed when using harmonic functions in the perturbation basis with wave-lengths corresponding to the structure domains (grey regions), this increases the error of the echo decay at q-values corresponding to such wave lengths. At such wave lengths the approximate eigenfunctions consist of linear combinations of eigenfunctions corresponding to the outer (white region) and inner (grey regions) domains. This effect can be minimized by increasing the number of surface modes M, preserving the orthogonality to the inner domains and or not introduce harmonic functions at the resonance points. Note that the error due to this resonance effect is of the same order as the error at other q-values in the geometries presented, but more pronounced.

The method share similarities with other methods formulated on the boundary such as the boundary element methods [33] (BEM), analytic element methods [34] (AEM) and boundary approximation methods [35,36] (BAE), also known as Trefftz methods, but might be an alternative due to the small size of the resulting perturbation matrix achieved in $O(s^2)$ time where s is the number of boundary elements. The approximate signals can also be improved by using the approximative eigenfunctions/eigenvalues as an initiator for other iterative method as for example [37] which relies on an initial guess of the eigenvalues. As the standard methods for calculations of the diffusion propagator are impractical for large-scale systems, due to the heavy computational demand, the mixed basis approach is suggested as a realistic tool for calculating approximative echo decays.

On a final note the mixed basis approach can perhaps also be extended from the SGP-limit to cover time-dependent gradients using the matrix formulation developed by Callaghan [38] based on a multiple propagator approach [39].

References

[1] D.S. Grebenkov, Nmr survey of reflected brownian motion, Reviews of Modern Physics 79 (2007) 1077.
[2] W.S. Price, NMR Studies of Translational Motion, Cambridge University Press, 2009.
[3] P.T. Callaghan, Principles of Nuclear Magnetic Resonance Microscopy, Oxford University Press, 1991.
[4] J.H. Simpson, H.Y. Carr, Diffusion and nuclear spin relaxation in water, Physical Review 111 (1958) 1201–1202 ([first] NMR applied on water to measure diffusion).
[5] D.W. Mccall, D.C. Douglass, E.W. Anderson, Self-diffusion studies by means of nuclear magnetic resonance spin-echo techniques, Berichte der Bunsengesellschaft fr physikalische Chemie 67 (1963) 336–340.
[6] E.O. Stejskal, Use of spin echoes in a pulsed magnetic-field gradient to study anisotropic, restricted diffusion and flow, The Journal of Chemical Physics 43 (1965) 3597–3604.
[7] H.Y. Carr, E.M. Purcell, Effects of diffusion on free precession in nuclear magnetic resonance experiments, Physical Review 94 (1954) 630–638 (first discussion of flow).
[8] M.D. Hürlimann, K.G. Helmer, T.M. Deswiet, P.N. Sen, Spin echoes in a constant gradient and in the presence of simple restriction, Journal of Magnetic Resonance: Series A 113 (1995) 260–264.
[9] P.N. Sen, M.D. Hürlimann, T.M. de Swiet, Debye–Porod law of diffraction for diffusion in porous media, Physical Review B 51 (1995) 601–604.
[10] W.S. Price, P. Stilbs, O. Söderman, Determination of pore space shape and size in porous systems using NMR diffusometry. beyond the short gradient pulse approximation, Journal of Magnetic Resonance 160 (2003) 139–143.
[11] D. Topgaard, O. Söderman, Experimental determination of pore shape and size using q-space NMR microscopy in the long diffusion-time limit, Magnetic Resonance Imaging 21 (2003) 69–76.
[12] J.E. Tanner, E.O. Stejskal, Restricted self-diffusion of protons in colloidal systems by the pulsed-gradient, spin-echo method, The Journal of Chemical Physics 49 (1968) 1768–1778.
[13] H.C. Torrey, Bloch equations with diffusion terms, Physical Review 104 (1956) 563–565.
[14] P.T.C.A. Coy, Pulsed gradient spin echo nuclear magnetic resonance for molecules diffusing between partially reflecting rectangular barriers, The Journal of Chemical Physics 101 (1994) 4599–4609.
[15] P. Linse, O. Soderman, The validity of the short-gradient-pulse approximation in nmr studies of restricted diffusion. simulations of molecules diffusing between planes, in cylinders and spheres, Journal of Magnetic Resonance: Series A 116 (1995) 77–86.
[16] L.Z. Wang, A. Caprihan, E. Fukushima, The narrow-pulse criterion for pulsed-gradient spin-echo diffusion measurements, Journal of Magnetic Resonance: Series A 117 (1995) 209–219.
[17] R. Mair, P. Sen, M. Hrlimann, S. Patz, D. Cory, R. Walsworth, The narrow pulse approximation and long length scale determination in xenon gas diffusion nmr studies of model porous media, Journal of Magnetic Resonance 156 (2002) 202–212.

[18] P.T. Callaghan, S.L. Codd, J.D. Seymour, Spatial coherence phenomena arising from translational spin motion in gradient spin echo experiments, Concepts in Magnetic Resonance 11 (1999) 181–202.
[19] P.T. Callaghan, A. Coy, T.P.J. Halpin, D. MacGowan, K.J. Packer, F.O. Zelaya, Diffusion in porous systems and the influence of pore morphology in pulsed gradient spin-echo nuclear magnetic resonance studies, The Journal of Chemical Physics 97 (1992) 651–662.
[20] A. Coy, P.T. Callaghan, Pulsed gradient spin-echo NMR experiments on water surrounding close-packed polymer spheres, Journal of Colloid and Interface Science 168 (1994) 373–379.
[21] S.L. Codd, S.A. Altobelli, A PGSE study of propane gas flow through model porous bead packs, Journal of Magnetic Resonance 163 (2003) 16–22.
[22] P. Callaghan, Pulsed-gradient spin-echo nmr for planar, cylindrical, and spherical pores under conditions of wall relaxation, Journal of Magnetic Resonance: Series A 113 (1995) 53–59.
[23] G.B. Arfken, H.-J. Weber, Mathematical Methods for Physicists, fourth (International) ed., Academic Press, 1995.
[24] M. Nordin, M.N. Jacobi, M. Nydén, Deriving time-dependent diffusion and relaxation rate in porous systems using eigenfunctions of the laplace operator, Journal of Magnetic Resonance 201 (2009) 205–211.
[25] M. Nordin, M. Nilsson-Jacobi, M. Nydén, A mixed basis approach to approximate the spectrum of Laplace operator, Paper Presented at the VI's Proceedings of Interdisciplinary Transport Phenomena, Volterra, Italy, 2009. arXiv:0909.0935v1.
[26] P.P. Ewald, Die berechnung optischer und elektrostatischer gitterpotentiale, Annalen der Physik 369 (1921) 253–287.
[27] L. Greengard, V. Rokhlin, A fast algorithm for particle simulations, Journal of Computational Physics 73 (1987) 325–348.
[28] T. Amisaki, Precise and efficient Ewald summation for periodic fast multipole method, Journal of Computational Physics 21 (2000) 1075–1087.
[29] C.H. Neuman, Spin echo of spins diffusing in a bounded medium, The Journal of Chemical Physics 60 (1974) 4508–4512.
[30] P. Callaghan, Pulsed-gradient spin-echo NMR for planar, cylindrical, and spherical pores under conditions of wall relaxation, Journal of Magnetic Resonance: Series A 113 (1995) 53–59.
[31] D.E. Woessner, NMR spin-echo self-diffusion measurements on fluids undergoing restricted diffusion, The Journal of Physical Chemistry 67 (1963) 1365–1367.
[32] J. Neyman, E.L. Scott, Statistical approach to problems of cosmology, Journal of the Royal Statistical Society: Series B (Methodological) 20 (1958) 1–43.
[33] P. Banerjee, The Boundary Element Methods, McGraw-Hill, 1994.
[34] O.D.L. Strack, Principles of the analytic element method, Journal of Hydrology 226 (1999) 128–138.
[35] Z.-C. Li, R. Mathon, P. Sermer, Boundary methods for solving elliptic problems with singularities and interfaces, SIAM Journal on Numerical Analysis 24 (1987) 487–498.
[36] Z. Li, The Trefftz method for the Helmholtz equation with degeneracy, Applied Numerical Mathematics 58 (2008) 131–159.
[37] Z.-C. Li, T.-T. Lu, H.-S. Tsai, A.H. Cheng, The Trefftz method for solving eigenvalue problems, Engineering Analysis with Boundary Elements 30 (2006) 292–308.
[38] P.T. Callaghan, A simple matrix formalism for spin echo analysis of restricted diffusion under generalized gradient waveforms, Journal of Magnetic Resonance 129 (1997) 74–84.
[39] A. Caprihan, L.Z. Wang, E. Fukushima, A multiple-narrow-pulse approximation for restricted diffusion in a time-varying field gradient, Journal of Magnetic Resonance: Series A 118 (1996) 94–102.